Functional evaluation of hemodynamic response during neural activation using optical microangiography integrated with dual-wavelength laser speckle imaging

Jia Qin
Lei Shi
Hequn Wang
Roberto Reif
Ruikang K. Wang

Functional evaluation of hemodynamic response during neural activation using optical microangiography integrated with dual-wavelength laser speckle imaging

Jia Qin, Lei Shi, Hequn Wang, Roberto Reif, and Ruikang K. Wang[*]
University of Washington, Department of Bioengineering, Seattle, Washington 98195

Abstract. Evaluation of spatiotemporal hemodynamic and metabolic responses during neural activation is crucial in studying brain function. We explore the use of a noninvasive multifunctional optical imaging system to measure these responses in a mouse brain upon electrically stimulated neural activation, with the cranium left intact. The system is developed by integrating an optical microangiography (OMAG) imaging system with a dual-wavelength laser speckle imaging (DW-LSI) system. The DW-LSI, running at an image acquisition speed of ~100 Hz, is used to extract the large-scale two-dimensional map, revealing the localized response of blood flow, hemoglobin concentration, and metabolic rate of oxygen change. Guided by DW-LSI, the OMAG is, however, used to image the response of individual blood vessels with its unique depth-resolved capability. We show that the integrated system is capable of investigating neural activation, thus is potentially valuable in the preclinical study of the mechanism of neurovascular coupling. © The Authors. Published by SPIE under a Creative Commons Attribution 3.0 Unported License. Distribution or reproduction of this work in whole or in part requires full attribution of the original publication, including its DOI. [DOI: 10.1117/1.JBO.19.2.026013]

Neural activation provides a platform for the study of brain functions. The changes in neuronal activity associated with changes in local blood flow and metabolic responses are a physiological hallmark in brain function exploration.[1] Currently, the evaluation of hemodynamic and metabolic responses in neural activation has become an effective tool for studying normal or pathological brain function. It is reported that the local blood flow and energy metabolism are anatomically restricted to specific activated areas in the brain.[2] In the process of neurovascular response due to neural activation, nerve tissue in localized brain area is thought to be nourished by sufficient substrates, such as glucose and oxygen, which are required for local energy metabolism. Several parameters, including but not limited to, the dynamic variations of cerebral blood flow (CBF), the concentrations of hemoglobin, and cerebral metabolic rate of oxygen ($CMRO_2$) are used as surrogate markers for neuronal activation in specific brain areas.[3,4]

The highly vascularized central nervous system is enclosed by connective tissue layers, collectively called meninges, in which perivascular nerves play a role in regulating vascular tone and perfusion. During regulation process, chemical signals that are released from activated perivascular nerves and astrocytes alter vascular tones in order to reconcile local variations of blood flow in brain activities.[5] The blood circulation within meninges play an important role in a number of neurological diseases and complications.[6,7]

The currently available optical intrinsic signal imaging has difficulties associated with revealing the hemodynamic and metabolic information.[8] To obtain such information, laser speckle contrast imaging (LSI)[9] [including multiwavelength two-dimensional (2-D) imaging] have been used for imaging neural activation in brain with a relative large field of view.[9,10] LSI method detects multiple interference of the reflected (or transmitted) wavelets, i.e., speckle patterns, using digital cameras,[9] similar to snapping a time series of 2-D pictures. In this way, LSI lacks depth information; thus it cannot resolve fine structural information from individual sublayers of cortical tissue. Among depth-resolved imaging techniques, optical microangiography (OMAG) is a label-free noninvasive imaging modality that can be used to obtain three-dimensional (3-D) blood perfusion map within microcirculatory tissue beds *in vivo*, based on Fourier-domain optical coherence tomography.[11] Doppler OMAG (DOMAG) is a functional extension to OMAG that is capable of imaging blood flow velocity within functional vessels.[12] However, due to its limited imaging speed (normally line scan rate <100 KHz), the temporal resolution for DOMAG is currently not sufficient to capture 3-D hemodynamic responses of CBF, which is usually in an order of seconds or less. Therefore, we believe that by combining LSI with DOMAG we will overcome the disadvantages of each individual technique, and provide complementary information which can be used to better evaluate brain function. In this letter, we report the development of a multifunctional imaging system, in which dual-wavelength LSI (DW-LSI) and DOMAG is integrated into one system for imaging functional CBF changes. We demonstrate that the system is able to generate dynamic images of functional CBF response to hindpaw stimulation, revealing not only regional but also depth-resolved information

---

*Address all correspondence to: Ruikang K. Wang, E-mail: wangrk@uw.edu

within the meningeal layer as well as within the somatosensory cortex.

The schematic of the integrated system is shown in Fig. 1(a), where DW-LSI (left) and OMAG (right) subsystems are separately marked. In the DW-LSI, two laser diodes ($\lambda_1 = 780$ and $\lambda_2 = 825$ nm) were employed. The collimated beams from the laser diodes were first combined coaxially by a dichroic beam splitter DBS$_1$, and then expanded before uniformly illuminating the sample at an incident angle of ~60 deg.[13] The backscattered light from the sample was collected by a zoom lens and then routed to a second DBS$_2$ to split into the lights of $\lambda_1 = 780$ and $\lambda_2 = 825$ nm, separately. Finally, the light from each wavelength was captured by two CMOS cameras (Basler A504k, Anrensburg, Germany), which were operated in synchrony. The exposure time of the camera was set to 10 ms, giving high contrast for speckle flow imaging.[4] Both cameras run at 100 frames per second (fps), with each frame consisting of 1000×1000 pixels. This imaging performance is superior to spatiotemporal resolution previously reported in terms of frame rate and affordable pixel numbers.[4,14,15] The field of view was set at ~6 × 6 mm², covering the dimensions of the contralateral side of the mouse brain (MB) [Fig. 1(b)]. The setting ensures that the speckle size (~22 μm) is approximately twice the pixel size (12 μm), maximizing the speckle contrast.[16]

For the DOMAG [Fig. 1(a)], a superluminescent diode (central wavelength 1310 nm, bandwidth 56 nm) was employed to illuminate the system, giving a theoretical axial resolution of ~13 μm in air. The light was divided into two paths using a 2 × 2 optical coupler. The light in one of the paths was transmitted toward a mirror in the reference arm, and the light in the other path was transmitted toward the MB in the sample arm. In the sample arm, the light was coupled into an optical system which includes a collimator, a pair of galvo scanners, and an objective lens with a 30-mm focal length, providing a lateral resolution of ~10 μm. The lights reflected from the sample and reference arms were recombined and transmitted to a home-built spectrometer. The A-scan imaging rate in this study was ~1.5 kHz, operated in repeated B-scan mode (MB scan) at 3 fps. Each B-scan contained 500 A-lines, covering ~2.2 mm on the sample. The total time required to acquire a MB-scan sequence necessary for data analysis was 42 s.

To integrate DW-LSI and DOMAG into one system, a dichroic beam splitter DBS$_0$ [Fig. 1(a)] was used to bridge the lights from individual systems.

The details of the animal preparation, including anesthetic procedures, have been previously described in Ref. 17. Briefly, the animal was kept stable in a custom made stereotaxic stage and lightly anesthetized with isoflurane (0.2 L/min O2, 0.8 L/min air). An incision of ~1.2 cm was made on the skin along the direction of sagittal suture and the frontal parietal and interparietal bones were exposed. It is worth mentioning that the mouse cranium was neither thinned nor opened for imaging. The animal was then positioned under the DW-LSI and OMAG imaging probe. Finally, we used electric stimulation for neural activation in contralateral brain through applying electrodes into the hindpaw.[8] The stimulation protocol consisted of 2-s prestimulus, 15-s stimulus with 0.5-mA current, 3-Hz pulse frequency and 3-ms pulse duration,[8] and 25-s poststimulus.

For the evaluation of brain hemodynamic and metabolic responses, several parameters were calculated from the images captured by the integrated system. First, the speckle contrast maps were calculated as a ratio of standard deviation to mean intensity, rendered by moving a 5×5 pixels binning window in the raw intensity image at $\lambda_1 = 780$ nm. The relative flow changes were then derived based on the model of spatial speckle contrast versus flow velocity.[18] Second, the concentration changes of oxygenated hemoglobin (HbO), deoxygenated hemoglobin (Hb), total hemoglobin (HbT), and CMRO$_2$ were estimated by using the images acquired at λ_1 (780 nm) and λ_2 (825 nm), respectively. A differential model, based on absorption at λ_1 and λ_2, was used to estimate the changes in HbO and Hb.[13,15] Subsequently, HbT was evaluated by summing HbO and Hb, revealing the amount of hemoglobin (unit: millimole) per liter in the blood. CMRO$_2$ was evaluated by employing the method described in Ref. 19 where baseline concentrations of Hb (40 μM) and HbT (100 μM) are assumed. From the LSI images, we identified two regions: region 1 (R1), where the percentage of change in CBF was in the range of 2% to 4%, and region 2 (R2) where the change in HbO was in the range of 2 to 3 μM. The two regions were then overlapped to localize
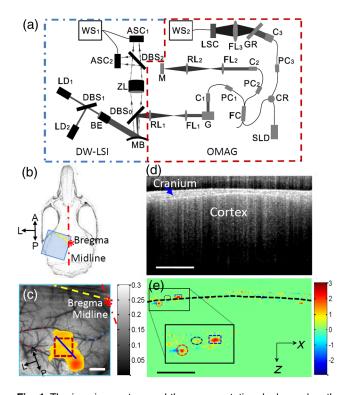

Fig. 1 The imaging system and the representative dual wavelength laser speckle imaging (DW-LSI) and Doppler optical microangiography (DOMAG) images. (a) The schematic of integrated DW-LSI (left) and DOMAG (right) system. LD: laser diode, DBS: dichroic beam splitter, BE: beam expander, ZL: zoom lens, ASC: area scan camera, WS: computer workstation, SLD: superluminescent diode, CR: circulator, FC: fiber coupler, PC: polarization controller, C: collimator, G: x–y galvanometer, FL: focusing lens, RL: relay lens, GR: grating, LSC: line scan camera, MB: mouse brain. (b) MB sketch, showing the area being imaged in the contralateral (left) side. (c) Somatosensory cortex region (SCR) (orange) identified by the DW-LSI approach, and superposed onto LSCI speckle contrast image, where Bregma is marked by asterisk, midline by dash-dotted line; coronal suture by dashed line. A: anterior, L: lateral, P: posterior. Scale bar = 1.0 mm. (d) Representative DOMAG B-scan of microstructures captured at the location marked by a line in (c); and (e) corresponding DOMAG phase map where the inset shows the enlarged three typical regions of interest. The cortical layer and meningeal layer are separated by the dashed line. Scale bar = 500 μm.

the activated region due the hindpaw stimulation, i.e., somatosensory cortex region (SCR) in the brain. After the SCR was localized, the OMAG probe was then guided to image vascular activations in detail within this region. A series of MB scans were captured and processed to provide cross-sectional blood flow images using the DOMAG algorithm, where the calculated phase difference values between adjacent A-lines of flow signals is used to estimate flow velocities.[12]

An entire mouse cranium is sketched in Fig. 1(b), where the imaging field ($6 \times 6 \text{ mm}^2$) is labeled by a shaded square at the contralateral side of the brain. The imaging results are given in Figs. 1(c)–1(e), respectively. In Fig. 1(c), the localized SCR is overlaid onto a typical speckle contrast vascular map. It is observed that typical branches of the middle cerebral artery (MCA) (marked by the red spots) and of the sagittal sinus (marked by the blue spots) are clearly visible. The branches arising from the MCA are responsible for supplying the sensorimotor cortex including the hind limb somatosensory cortex.[20] Veins on the cortical surface are responsible for draining the SCR into the superior sagittal sinus. It is notable that our identified SCR is localized within arteriole anastomotic region between MCA and anterior cerebral artery branches over the cortex, agreed with the prior report in Ref. 20.

After SCR was identified by the DW-LSI approach, the DOMAG was then guided into this region for some detailed investigation of blood flow responses in the individual vessels. Figure 1(d) presents one representative B-scan image within the DOMAG structural volume, where typical morphological features, such as cranium and cortex, are clearly visualized. The corresponding DOMAG phase map acquired during the stimulus is demonstrated in Fig. 1(e), with the positive value indicating that the flow is along the direction of incident light [z direction in Fig. 1(e)], otherwise opposite direction. We evaluated the hemodynamic responses of three regions of interest (ROI), marked in Fig. 1(e), including a large meningeal vein (diameter: $\sim 90 \ \mu m$, marked by square), a middle size meningeal artery (diameter: $\sim 40 \ \mu m$, marked by oval), and a cortical arterial (diameter: $\sim 50 \ \mu m$, marked by circle). In order to show hemodynamic responses due to the hindpaw stimulation, the summed phase difference values within each ROI were first accumulated over time, and then plotted over the time course.

Figure 2(a) shows the time course of the changes in CBF, $CMRO_2$, HbO, Hb, and HbT within a square region localized in the somatosensory area [Fig. 1(c)] before, during, and after electrical stimulation. As shown, apart from the concentration of Hb, all other measured parameters rise to a peak value at about the same time (~ 17 s) after the stimulation. The maximum decrease of Hb is observed behind the ridge wave of hyperemia; however, the change of Hb is not as obvious as those of other parameters. These trends are consistent with what was observed in Ref. 4. Note that an artery was situated within the SCR in our study while a vein was covered in Ref. 4. In addition, the peak change in CBF is observed greater than that in $CMRO_2$, indicating uncoupling between them, similar to that observed in other brain activation studies.[21] It is also interesting that HbO, HbT, and CBF show a secondary increase, probably due to a delayed stress relaxation in the blood vessels.[22] To better analyze the recovery period, zoomed-in views of the relative changes of CBF, HbO, and Hb during a 3.2-s time course after the stimulation are presented in Figs. 2(c) and 2(d), respectively. By the use of simple Fourier transform on the curves in
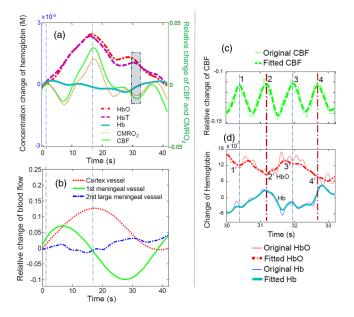

Fig. 2 (a) Time courses of the changes in cerebral blood flow (CBF), $CMRO_2$, HbO, Hb, and HbT for the SCR before, during, and after electrical stimulation. (b) DOMAG flow changes in specific vessels marked in Fig. 1(e). Zoomed-view of the curves in (a) (marked by rectangular box) indicates a pulsatile trend of (c) CBF and (d) HbO and Hb. 1′ to 4′ denoted in (d) correspond to 1 to 4 in (c).

Figs. 2(c) and 2(d), we estimated that the pulsatile frequency and respiratory frequency to be ~ 7.5 and ~ 1.2 Hz, respectively. These observations demonstrate that the current system is able to record and recognize the patterns of pulsatile oscillation and respiratory.

Figure 2(b) shows the time course of flow changes for the three typical vessels [see Fig. 1(d)], evaluated by DOMAG, where the results shown were first low-pass filtered and then the pulsatile and respiratory frequencies eliminated. Flow changes in the three vessels investigated are obvious. It is observed that the cortical arterial [marked by dotted line in Fig. 2(b)] performs the hemodynamic reconciling with the hyperemia exhibited by the DW-LSI. The timings for the peak values to occur are consistent between OMAG and DW-LSI. However, the big meningeal vessel [dash-dotted line in Fig. 2(b)] exhibits a totally different flow response compared to that in the cortical vessel, where almost no flow change in the big meningeal vessel was observed throughout the stimulus procedure. For these reasons, this big meningeal vessel is probably a vein, which has no significant response during the stimulation.[23,24] It is also very interesting to see that the CBF in another meningeal artery [solid line in Fig. 2(b)] shows an oscillating pattern, which may be caused by stimulated vascular tone.[5] Overall, the integrated imaging system has the capability to provide spatial and temporal details of the hemodynamic and metabolic responses throughout the neural activation procedure.

In summary, we have shown that the proposed multifunctional imaging system is useful in delineating the microvascular hemodynamic and metabolic responses during neural activation, delivering complementary information regarding 2-D functional maps of microvasculature (offered by DW-LSI) and depth-resolved flow responses within individual blood vessels (enabled by OMAG). We expect that this integrated system can be applied to any rodent models with local CBF and oxygenation

variations, promising the exploration of a broad range of brain disorders, such as stroke and cerebral thrombosis, etc.

Acknowledgments

References

1. K. K. Kwong et al., "Dynamic magnetic resonance imaging of human brain activity during primary sensory stimulation," *Proc. Natl. Acad. Sci. U. S. A.* **89**(12), 5675–5679 (1992).
2. G. Bonvento, N. Cholet, and J. Seylaz, "Sustained attenuation of the cerebrovascular response to a 10 min whisker stimulation following neuronal nitric oxide synthase inhibition," *Neurosci. Res.* **37**(2), 163–166 (2000).
3. B. M. Ances, "Coupling of changes in cerebral blood flow with neural activity: what must initially dip must come back up," *J. Cereb. Blood Flow Metab.* **24**(1), 1–6 (2004).
4. A. K. Dunn et al., "Simultaneous imaging of total cerebral hemoglobin concentration, oxygenation, and blood flow during functional activation," *Opt. Lett.* **28**(1), 28–30 (2003).
5. E. Hamel, "Perivascular nerves and the regulation of cerebrovascular tone," *J. Appl. Physiol.* **100**(3), 1059–1064 (2005).
6. A. F. McCaslin et al., "In vivo 3D morphology of astrocyte-vasculature interactions in the somatosensory cortex: implications for neurovascular coupling," *J. Cereb. Blood Flow Metab.* **31**(3), 795–806 (2010).
7. H. Bolay et al., "Intrinsic brain activity triggers trigeminal meningeal afferents in a migraine model," *Nat. Med.* **8**(2), 136–142 (2002).
8. Y. Chen et al., "Optical coherence tomography (OCT) reveals depth-resolved dynamics during functional brain activation," *J. Neurosci. Methods* **178**(1), 162–173 (2009).
9. D. A. Boas and A. K. Dunn, "Laser speckle contrast imaging in biomedical optics," *J. Biomed. Opt.* **15**(1), 011109 (2010).
10. V. Kalchenko et al., "Label free in vivo laser speckle imaging of blood and lymph vessels," *J. Biomed. Opt.* **17**(5), 050502 (2012).
11. L. An, J. Qin, and R. K. Wang, "Ultrahigh sensitive optical microangiography for in vivo imaging of microcirculations within human skin tissue beds," *Opt. Express* **18**(8), 8220–8228 (2010).
12. R. K. Wang and L. An, "Doppler optical micro-angiography for volumetric imaging of vascular perfusion in vivo," *Opt. Express* **17**(11), 8926–8940 (2009).
13. J. Qin et al., "Fast synchronized dual-wavelength laser speckle imaging system for monitoring hemodynamic changes in a stroke mouse model," *Opt. Lett.* **37**(19), 4005–4007 (2012).
14. E. M. C. Hillman, "Optical brain imaging in vivo: techniques and applications from animal to man," *J. Biomed. Opt.* **12**(5), 051402 (2007).
15. Z. C. Luo et al., "Simultaneous imaging of cortical hemodynamics and blood oxygenation change during cerebral ischemia using dual-wavelength laser speckle contrast imaging," *Opt. Lett.* **34**(9), 1480–1482 (2009).
16. S. J. Kirkpatrick et al., "Detrimental effects of speckle-pixel size matching in laser speckle contrast imaging," *Opt. Lett.* **33**(24), 2886–2888 (2008).
17. Y. Jia, N. Alkayed, and R. K. Wang, "Potential of optical microangiography to monitor cerebral blood perfusion and vascular plasticity following traumatic brain injury in mice in vivo," *J. Biomed. Opt.* **14**(4), 040505 (2009).
18. R. Bandyopadhyay et al., "Speckle-visibility spectroscopy: a tool to study time-varying dynamics," *Rev. Sci. Instrum.* **76**(9), 1–11 (2005).
19. A. K. Dunn et al., "Spatial extent of oxygen metabolism and hemodynamic changes during functional activation of the rat somatosensory cortex," *Neuroimage* **27**(2), 279–290 (2005).
20. A. J. Kennerley et al., "Vascular origins of BOLD and CBV fMRI signals: statistical mapping and histological sections compared," *Open Neuroimaging J.* **4**, 1–8 (2010).
21. P. T. Fox and M. E. Raichle, "Focal physiological uncoupling of cerebral blood flow and oxidative metabolism during somatosensory stimulation in human subjects," *Proc. Natl. Acad. Sci. U. S. A.* **83**(4), 1140–1144 (1986).
22. A. M. VanDijk et al., "Mechanics of resting isolated single vascular smooth muscle cells from bovine coronary artery," *Am. J. Physiol.* **246**(3 Pt 1), C277–287 (1984).
23. H. Betz, "Traumatic arteriovenous fistula between the middle meningeal artery and vein. Spontaneous regression trend during angiographic controls," *Der Radiologe* **14**(12), 528–531 (1974).
24. M. Kurosawa et al., "Increase of meningeal blood flow after electrical stimulation of rat dura mater encephali: mediation by calcitonin gene-related peptide," *Br. J. Pharmacol.* **114**(7), 1397–1402 (1995).

Biographies of the authors are not available.